Journal of Structural Engineering & Applied Mechanics (2025) 8(4):312-330
DOI 10.31462/jseam.2025.04312330

RESEARCH ARTICLE

Impact of scaled and non-scaled earthquake records on the seismic performance of reinforced concrete buildings

Gökhan Dok[1*], Ali Bertu Sağlam[1]

[1] Sakarya University of Applied Sciences, Department of Civil Engineering, Sakarya, Türkiye

Article History

Received 23 October 2025
Accepted 17 December 2025

Keywords

Turkish building earthquake code
Earthquake records
Scaling
Nonlinear analysis
Reinforced-concrete high-rise buildings

Abstract

In this study, the effect of earthquake record scaling on the seismic behavior of high-rise reinforced concrete structures was investigated within the scope of the Turkish Building Earthquake Code (TBEC-2018). A 27-story reinforced concrete building with a shear wall–frame structural system was analyzed using both linear and nonlinear methods. In the linear analysis phase, the structural design was carried out according to the strength-based design approach (SBD) and the modal combination method defined in TBEC-2018. In the nonlinear analyses, the deformation-based assessment (DBA) approach was adopted, and nonlinear time-history analyses (NTHA) were performed. Eleven real earthquake records were scaled in accordance with the horizontal elastic design spectrum defined for the DD-1 earthquake level (the maximum considered earthquake with a 2% probability of exceedance in 50 years, corresponding to a return period of 2475 years) and the requirements of TBEC-2018 using the simple scaling method. The results obtained from the analyses performed with both scaled and unscaled earthquake records were evaluated in terms of relative story drifts, base shear forces, plastic rotation demands, and unit deformations in structural walls. The findings indicate that scaled earthquake records significantly influence deformation demands and the energy dissipation capacity of high-rise buildings. Moreover, the results suggest that the applicability of the performance limit values defined in TBEC-2018 to nonlinear analyses of tall buildings should be further examined.

1. Introduction

Earthquakes are natural phenomena that occur as a result of the sudden release of elastic energy accumulated in the Earth's crust, often causing severe damage to the load-bearing systems of structures [1, 2]. Türkiye is located on the Alpine-Himalayan seismic belt, and approximately 92% of its land area is exposed to seismic risk [3]. Consequently, earthquake-resistant design and the performance assessment of the existing building stock represent one of the primary research fields within the practice of civil engineering in Türkiye [4, 5]. Earthquake-resistant design aims to ensure that structures maintain a specified performance level under seismic loading without experiencing collapse. The relevant design codes define the expected behavior of structural systems and impose limits on ductility, stiffness, and energy dissipation capacity [6]. The current Turkish Building Earthquake Code (TBEC-2018) introduced significant advancements over the 2007 version

* Corresponding author (gokhandok@subu.edu.tr)
eISSN 2630-5763

by adopting a performance-based design philosophy [7]. Among these innovations are the introduction of multiple earthquake hazard levels (DD-1, DD-2, DD-3, DD-4), special design provisions for high-rise buildings, and the mandatory use of nonlinear time-history analyses [8]. These levels represent varying probabilities of exceedance for a 50-year period, corresponding to different return periods [1]. According to the Turkish Building Earthquake Code (TBEC-2018), four earthquake ground motion levels are defined: DD-1 (Maximum Considered Earthquake – 2% probability of exceedance in 50 years, 2475-year return period), DD-2 (Design Earthquake – 10% probability, 475 years), DD-3 (Frequent Earthquake – 50% probability, 72 years), and DD-4 (Service Earthquake – 68% probability, 43 years). In high-rise buildings (Building Height Class, BHC = 1), the dynamic behavior of the structure is closely related to modal participation ratios, interstory drifts, and the fundamental period obtained through modal combination methods [9]. However, the degree to which response spectra used in linear analyses represent actual ground motions introduces uncertainty in performance predictions [10]. Therefore, the use of scaled earthquake records in nonlinear time-history analyses has become increasingly preferred in seismic engineering applications [11]. The scaling of earthquake records refers to the process of adjusting recorded ground motions so that their response spectra conform to the design spectrum defined by the relevant code. This adjustment is typically carried out within a specific period range (e.g., 0.2–1.5T), ensuring that the amplitudes of the records adequately match the target spectrum [12, 13]. Such an approach preserves the frequency content of real earthquakes, resulting in more realistic structural responses [14]. Previous studies have demonstrated that analyses conducted with scaled records significantly influence structural responses such as peak displacements, base shear forces, and the formation of plastic hinges [15–17]. Nonlinear analysis methods play a crucial role in evaluating the seismic response of high-rise structures. Nonlinear Time-History Analysis (NTHA) allows for the consideration of material nonlinearity and plastic hinge development, enabling a realistic assessment of structural behavior under dynamic loading [18]. This method provides reliable results for determining performance levels and evaluating the influence of scaled earthquake records on structural response, particularly in tall buildings [19, 20]. In this study, the effect of scaled earthquake records on the seismic behavior of a 27-story reinforced concrete shear wall–frame structure was investigated within the scope of TBEC-2018. The primary objective is to evaluate how records obtained through simple scaling influence the outcomes of linear and nonlinear analyses—such as interstory drift ratios, base shear forces, plastic rotations, and shear wall deformations—and to discuss the adequacy of the performance limit values prescribed by TBEC-2018.

2. Material and methodology

In this study, the nonlinear time-history analysis was employed to evaluate the seismic behavior of reinforced concrete high-rise buildings in accordance with the Turkish Building Earthquake Code (TBEC-2018) [1]. The case study structure is a 27-story reinforced concrete shear wall–frame system modeled based on the soil conditions of the Kaynarca district in Sakarya Province. The research primarily focuses on assessing the influence of scaled earthquake records on the seismic response of high-rise buildings. Furthermore, the study presents a detailed explanation of the analysis procedure, including the determination of effective section flexural stiffness, selection of earthquake records, scaling methodology, and subsequent analysis stages.

2.1. Structural models

The structure was modeled in three dimensions using the finite element software Sap2000 v23 [21]. The structural system consists of reinforced concrete shear walls and frames arranged symmetrically in both the X and Y directions. The concrete and reinforcing steel grades were defined as C40 and B420C, respectively. The analyzed building comprises 27 stories, including two basement levels below the ground floor. The story height was set to 3.0 m for all levels, resulting in a total building height of 75 m. The structure was classified as a residential high-rise building according to its intended use. The building has a plan area of 28×23 m, and its load-bearing system follows a symmetrical shear wall–frame configuration. The dimensions of structural members vary along the building height. For the first nine stories, the column sections were designed as 130×130 cm, while 100×100 cm sections were used for the upper stories. The longitudinal reinforcement ratio of the columns was ρ = 0.023, with a bar diameter of Ø26 mm and transverse reinforcement of Ø12 mm. All shear walls were modeled with a constant thickness of 60 cm throughout the building height. The longitudinal reinforcement ratio in the walls was defined as ρ = 0.002, using Ø16 mm longitudinal bars and Ø12 mm confinement reinforcement. The majority of the beam elements were designed with cross-sectional dimensions of 40×70 cm, incorporating Ø22 mm longitudinal reinforcement, a transverse reinforcement ratio of ρ = 0.014, and Ø12 mm stirrups. In the analytical model, floor slabs were not explicitly modeled as shell elements; instead, their effects were represented through equivalent distributed surface loads applied to the beams. The three-dimensional structural model and the cross-sectional dimensions of the primary load-bearing elements are illustrated in Fig. 1.

The story plan of the building is identical across all stories and is presented in Fig. 2. To accurately represent the stiffness characteristics of the columns and shear walls, the effective flexural stiffness (EIeff.) values were determined in accordance with the provisions of TBEC-2018 and the recommendations available in the literature [22–24]. The effective flexural stiffness is one of the most critical parameters used to approximate the nonlinear behavior of reinforced concrete members. Accurate representation of stiffness has a direct influence on the natural vibration periods, modal mass participation factors, and the distribution of seismic forces within the structure [22].

According to the analysis results, the fundamental periods in the X and Y directions were found to be nearly identical, and the number of modes required to achieve over 95% cumulative mass participation was the same in both directions. The period values and modal participation of mass in the X direction were illustrated in Fig. 3, and values were given in Table 1. Previous studies have demonstrated that the post-cracking stiffness ratios of beam and column elements vary depending on material strength, reinforcement ratio, and cross-sectional geometry [23, 24].

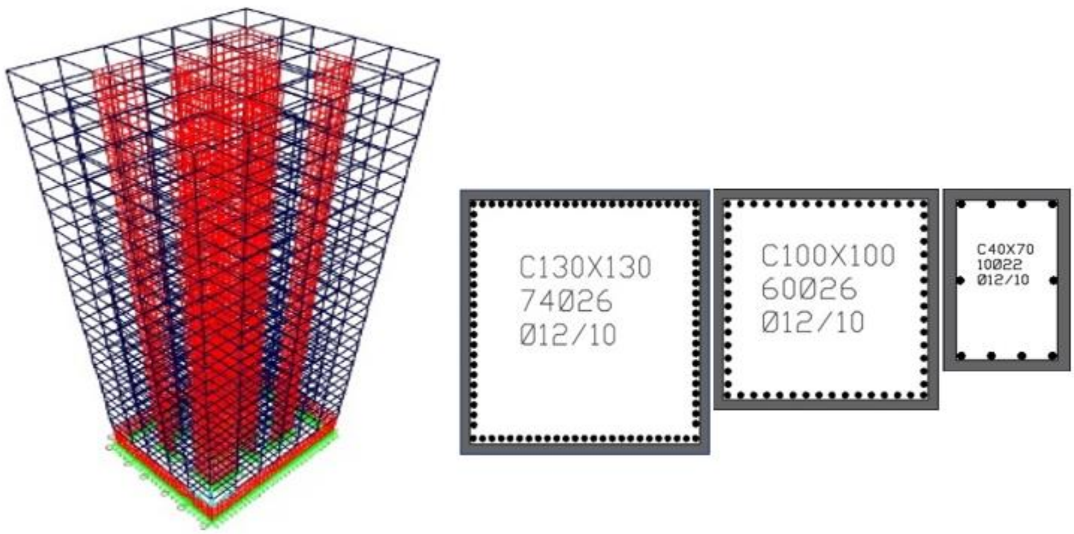

Fig. 1. 3D structural models and cross-sectional details of structural elements

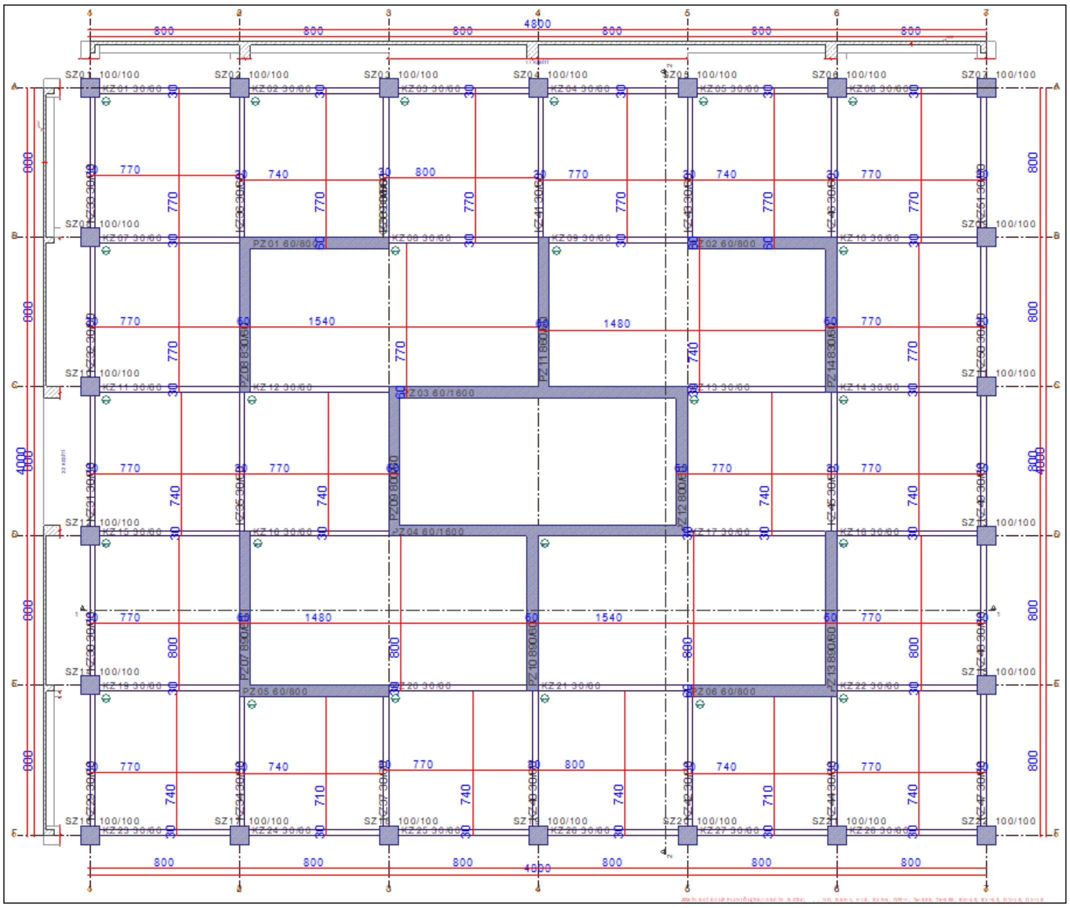

Fig. 2. The plan view of the stories (dimension in cm)

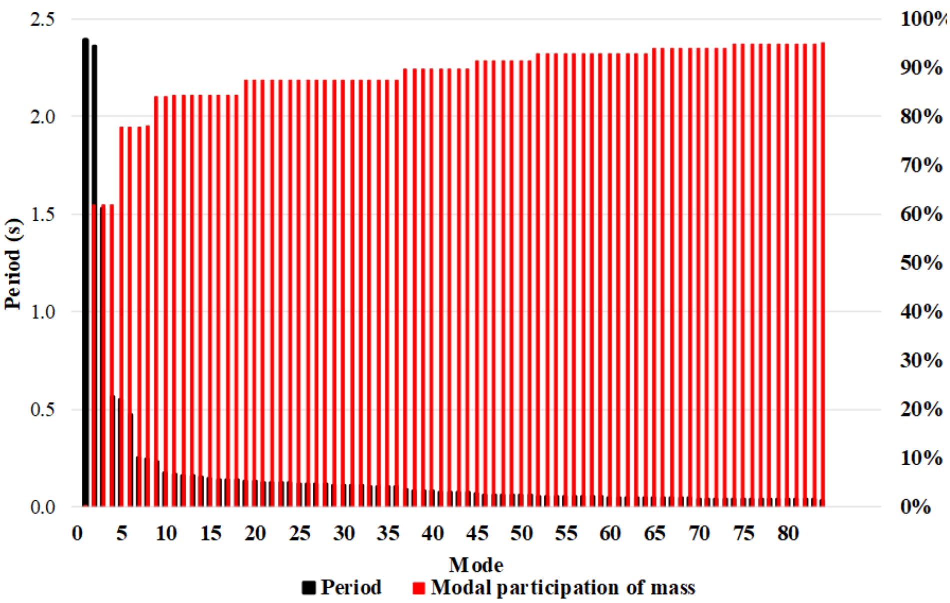

Fig. 3. The period values and modal participation of mass in the X direction

Table 1. Period values and modal participation mass ratios

Mod	Period	UX	UY	∑ UX	∑UY
1	2.39	0.0002	0.622	0.0002	0.622
2	2.38	0.620	0.0002	0.621	0.622
.	.	.	.	.	.
.	.	.	.	.	.
.	.	.	.	.	.
84	0.03	0.0002	0.0002	0.953	0.958

In this study, the effective flexural stiffness of columns and beams was obtained by multiplying the initial stiffness by factors of 0.70 and 0.35, respectively, in accordance with TBEC-2018. For the shear behavior of these members, no reduction was applied as specified in the code. For reinforced concrete shear walls, a reduction factor of 0.50 was used for both flexural and shear stiffness. All these values were adopted in the design stage, while for the evaluation stage, the stiffness values were determined using the relationship given in Eq. (1) of TBEC-2018, as stated in Section 5.4. In these equations, L_s M_y, and θ_y represent the shear span, yield moment, and yield rotation, respectively.

$$(\mathrm{EI})_{\mathrm{e}} = \frac{\mathrm{M}_y}{\theta_y}\frac{L_s}{3} \tag{1}$$

A real building was not used as the case study model. Instead, the building was assumed to be designed and constructed in accordance with TBEC-2018 for a site located in Sakarya Province. To accurately evaluate the structural behavior under seismic effects, the regional seismic parameters were determined based on the provisions of the Turkish Building Earthquake Code [1]. The site was assumed to be located in the Kaynarca district of Sakarya, with coordinates latitude 41.0360162° and longitude 30.3025914°, and a soil classification of ZD. For the DD-2 earthquake level, as defined in TBEC-2018 and the Türkiye Earthquake Hazard Map (Disaster and Emergency Management Authority, AFAD, 2022), the map spectral acceleration coefficients were obtained as $S_s = 0.727$ for a short period (0.2 s) and $S_1 = 0.209$ for one second (1.0 s). Based on these parameters, the design spectral acceleration coefficients were calculated as SDS = 0.886 (short-period) and $S_{D1} = 0.456$ (one-second period). For the DD-1 earthquake level, the corresponding coefficients were Ss = 1.314 and S1 = 0.360, yielding $S_{DS} = 1.314$ and $S_{D1} = 0.698$. Using these values, the horizontal elastic acceleration spectra for different earthquake levels were computed according to the spectrum defined by TBEC-2018, as illustrated in Fig. 4.

The building is classified as occupancy class BOC = 3 (building occupancy class) and building importance factor 1 (BIF), which corresponds to residential buildings according to TBEC-2018. Considering the total height and structural characteristics, the Building Height Class (BHC) was defined as BHC = 1, applicable to reinforced concrete buildings exceeding 60 m in height, where special analysis methods must be used to capture high-rise structural behavior. Based on the computed SDS and SD1 parameters, the Seismic Design Category (SDC) of the structure was determined as SDC = 1, indicating that the building is located in a region with the highest level of seismic hazard. According to TBEC-2018, the Nonlinear Time-History Analysis (NTHA) method is mandatory for the seismic evaluation of high-rise buildings. In determining performance levels, the earthquake design levels defined in the code—DD-1 and DD-2—were considered: For the DD-2 (Design Earthquake) level, the target performance level was defined as Controlled Damage (CD); for the DD-1 (Maximum Considered Earthquake) level, the target performance level was defined as Collapse Prevention (CP). These parameters formed the basis for developing the design acceleration spectrum used in both linear and nonlinear analyses and for selecting and scaling the ground motion records. A summary of all the parameters used in the analyses is provided in Table 2. The DD-1 level corresponds to an earthquake with a 2% probability of exceedance in 50 years (recurrence period of 2475 years), representing the maximum considered earthquake. The DD-2 level represents an earthquake with a 10% probability of exceedance in 50 years (recurrence period of 475 years), commonly referred to as the design earthquake. In this study, the characteristic compressive strength of concrete was taken as 40 MPa (C40), while B420C reinforcing steel with a yield strength of 420 MPa and an ultimate tensile strength of 500 MPa was used.

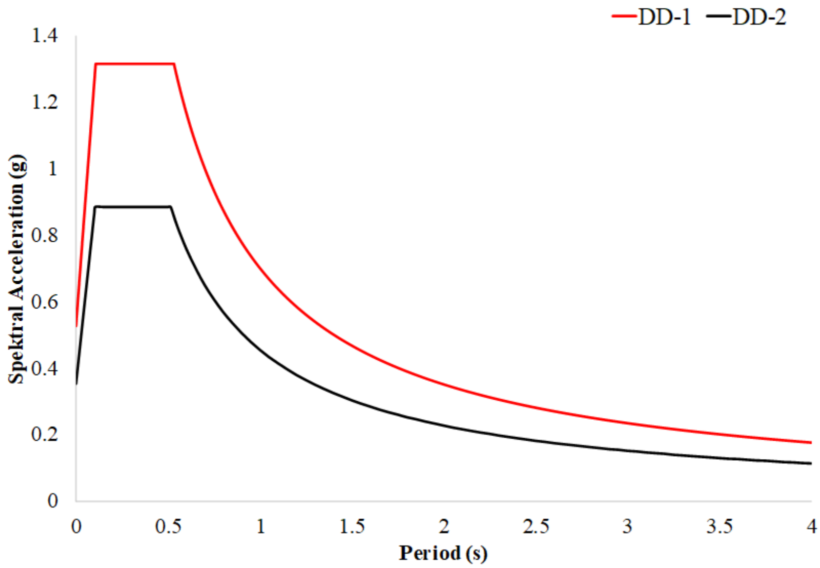

Fig. 4. TBEC 2018 horizontal elastic acceleration spectrum [1]

Table 2. Analysis Parameters

Parameters	Values
Number of stories	27
Soil class	ZD
Concrete	C40
Reinforcement	B420C
Ss (DD-1)	1.314
S1 (DD-1)	0.360
SDS (DD-1)	1.314
SD1 (DD-1)	0.698
BOC	3.0
BIF	1.0
BHC	1.0
SDC	1.0
Per. Target (DD-1)	CP

In the structural modeling, both dead loads (self-weight and superimposed permanent loads) and live loads were considered. The self-weight of the reinforced concrete elements was automatically included by the analysis software. In addition, a uniformly distributed dead load of 25 kN/m (including self-weight) and a live load of 2 kN/m were applied equally to all beams. For the reinforced concrete building with plan dimensions of 28×23 m, a total floor load of approximately 13.75 kN/m², corresponding to the combination (G + 0.3Q), was taken into account in the gravity load and mass calculations. The load combinations were defined in accordance with TBEC-2018 and Turkish Standards 498: Design loads for buildings (TS 498) [26], consistent with standard design practice.

2.2. Selection and scaling of earthquake records

For the nonlinear time-history analyses, a total of 11 real ground motion records representing different earthquake hazard levels were selected. The earthquake data were obtained from the Pacific Earthquake Engineering Research Center (PEER) Strong Motion Database [27] and the AFAD TADAS (Disaster and Emergency Management Authority – Strong Ground Motion Archive) web-based platform [28]. During record selection, seismotectonic characteristics similar to those of the study region—such as moment magnitude, fault mechanism, and site class—were taken into consideration [25]. The principal parameters of the selected ground motions, including peak ground acceleration (PGA), year, focal mechanism, shear wave velocity ($V_{S_{30}}$), moment magnitude (M_w), station, Rrup., and scale factor, are summarized in Table 3.

The selected earthquake records were scaled using a simple scaling method so that their spectra matched 1.3 times the horizontal elastic design spectrum defined for the DD-1 earthquake level. The scaling process was performed in accordance with TBEC-2018, ensuring that the spectral accelerations of the scaled records were not lower than those of the design spectrum within the period range of 0.2T to 1.5T, where T denotes the fundamental period of the structure. In this method, the frequency content of the original records remains unchanged, while only the amplitudes are adjusted to fit the target spectrum [5]. The acceleration–time histories of the selected ground motions are illustrated in Fig. 5.

Table 3. Strong ground motion parameters

Earthquake	PGA (g)	Year	Focal mechanism	Shear wave velocity V_{S30} (m/s)	Moment Magnitude (M_w)	Station	Rrup.	Scale factor
Bingol	0.52	2003	Strike-slip	529	6.4	TK1201	5.8	1.7
ChiChi	0.74	1999	Reverse Oblique	704.6	7.6	TCU045	26	1.5
Kocaeli	0.48	1999	Strike-slip	412	7.6	TK5401	5.9	3.8
Duzce	0.82	1999	Strike-slip	294	7.1	TK1401	8.6	4.2
Elmayor6051	0.63	2010	Reverse	380.6	7.2	Mountain Center	128.7	1.1
Elmayor6056	0.52	2010	Reverse	387.1	7.2	Mill Creek Ranger	198.6	1
Erzincan	0.72	1992	Strike-slip	455	6.6	TK2402	16.8	1.68
Loma-Prieta	0.85	1989	Reverse Oblique	391.9	6.9	APEEL 10 - Skyline	41.9	1.68
L-Aquila	0.51	2009	Normal	328.6	6.3	Termoli	122	1.65
Landers	0.60	1992	Strike-slip	379.3	7.3	Joshua Tree	11	4.5
Northridge	0.75	1994	Reverse	549.8	6.7	Anacapa Island	36.8	1.8

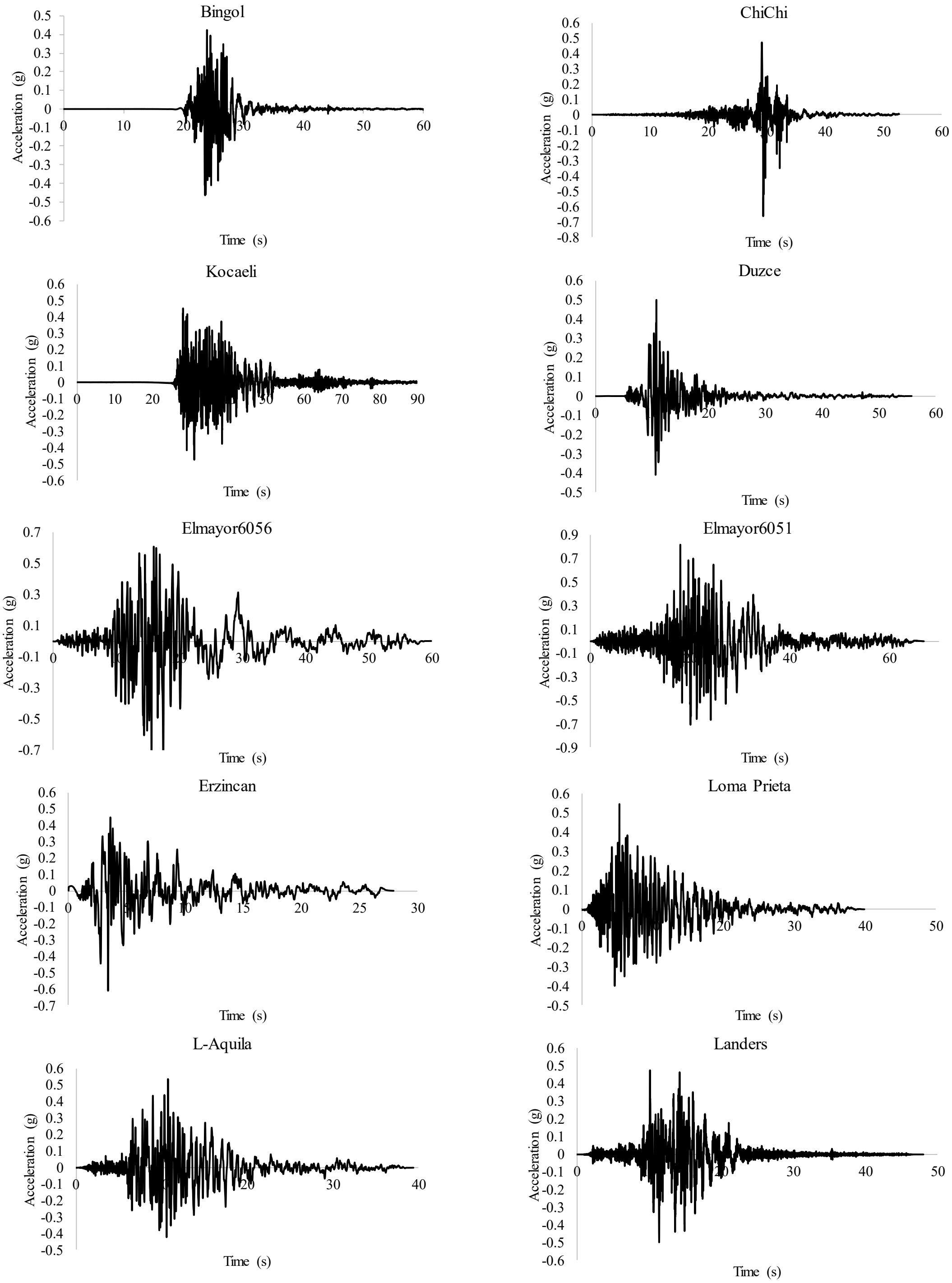

Fig. 5. Acceleration-time relationships of strong ground motions

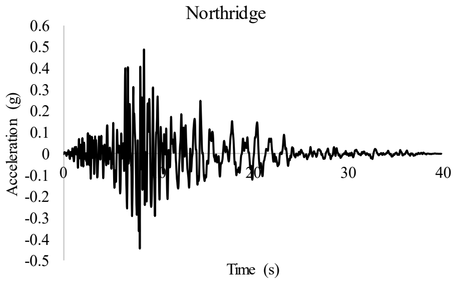

Fig. 5. Continued

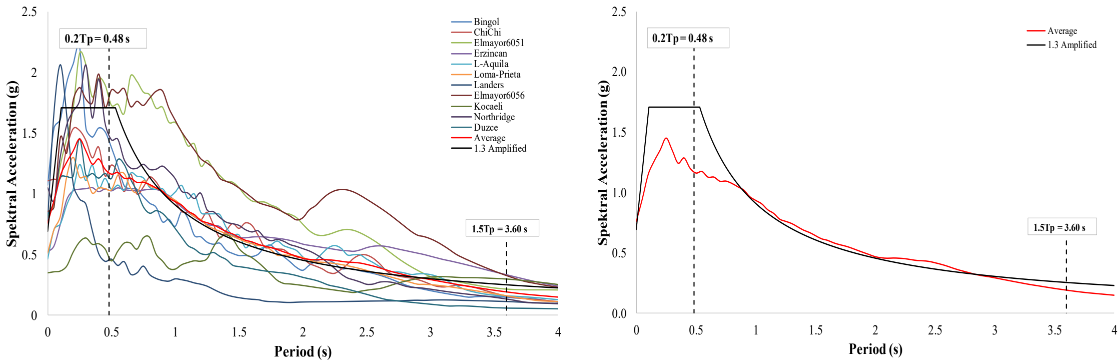

(a)

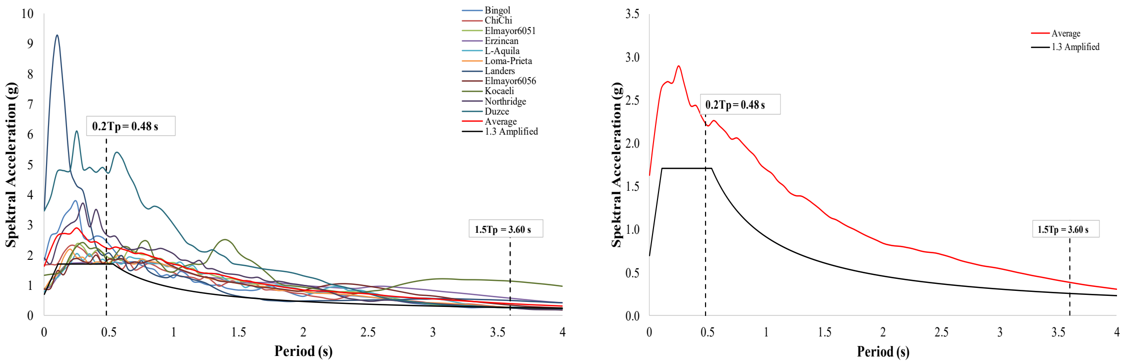

(b)

Fig. 6. Acceleration response spectrums of a) non-scaled and b) scaled strong ground motions

Following the scaling procedure, separate analyses were conducted using both the original (unscaled) and scaled records. The results were compared in terms of interstory drift ratios, base shear forces, plastic rotations, and shear strain demands in the structural walls. These analyses aimed to assess the influence of record scaling on the energy dissipation capacity and deformation demands of the high-rise structure [6, 11, 14, 25]. An average response spectrum was obtained by taking the arithmetic mean of the acceleration spectra derived from the scaled ground motion records, as illustrated in Fig. 6.

In this study, 11 ground motion records obtained from the PEER database and the AFAD TADAS (Disaster and Emergency Management Authority – Strong Ground Motion Archive) platform were applied in the X direction. According to TBEC-2018, both horizontal components of each ground-motion record must be applied simultaneously; furthermore, when single-component analyses are reported, the records should be rotated to the orthogonal direction so that both components are considered. Therefore, for the set of 11 records used in this study, a total of 22 analyses (11 records×2 orthogonal directions) would be required. In the present study, however, modal analysis showed that the dynamic characteristics in the X and Y directions are very similar; accordingly, and for the sake of clarity in presentation, the numerical analyses were performed and reported for the X direction only, and the results were compared on that basis. It was observed that, after scaling the earthquake records used in this study, the resulting acceleration spectra and the mean acceleration spectrum derived from them notably exceeded the design spectrum across the wide-period range. This outcome can be explained as follows: the average response spectrum obtained from the scaled records generally conforms to the TBEC-2018 target spectrum within the 0.2 T_p to 1.5T_p period range. However, some individual records exhibit noticeably lower spectral accelerations than the design spectrum, particularly within the 0.5–1.0 s and 2.5–3.6 s ranges. Consequently, relatively large scale factors were required for those records to achieve spectral compatibility. While these adjustments bring the lower portions of the spectra closer to the target, they also amplify the spectral ordinates in regions that were already near or slightly above the design spectrum. Therefore, additional re-scaling would not yield a meaningful improvement and could instead distort the overall spectral balance.

2.3. Numerical study

In the linear analysis of the structure, a Strength Design (SD) approach was adopted through a preliminary design process, and the seismic loads were determined using the Modal Response Spectrum (MRS) method. The irregularity checks, importance factor, building height class, and seismic design category were defined in accordance with the provisions of Chapter 4 of the TBEC-2018. For nonlinear analyses, the Deformation-Based Assessment (DBA) approach was implemented, employing Nonlinear Time History Analysis (NTHA) as the primary evaluation method. The nonlinear dynamic analyses were conducted using step-by-step Newmark time integration. In this study, Rayleigh damping was adopted. The mass-proportional and stiffness-proportional coefficients were defined by assuming a constant 2.5% damping ratio for the first two fundamental modes in the evaluated direction. In this context, plastic hinges were assigned to beams and columns, while fiber-section models were utilized for shear walls. The confined concrete model defined in TBEC-2018 and an elastic–perfectly plastic steel model were adopted to represent the nonlinear material behavior [18, 21, 23]. The material models used in the analyses are illustrated in Fig. 7.

The first step of the nonlinear analysis involves defining the nonlinear material properties of structural components. Accordingly, the material models specified in TBEC-2018 were employed in this study. To determine the sectional behavior of structural members, the XTRACT software [29] was utilized to obtain moment–curvature (M–φ) relationships for each element. Since the structural system is primarily a frame-type system, the concentrated plastic hinge approach was adopted for modeling nonlinear behavior. In this regard, P–M_2–M_3 interaction-based plastic hinges were defined for columns, while plastic hinges were assigned only in the M_3 direction for beams.

Based on the defined material models, plastic rotation and deformation limits were determined in accordance with Chapter 5 of the Turkish Building Earthquake Code (TBEC-2018). These limit values were derived from the moment–curvature ($M - \varphi$) relationships obtained using the material models illustrated in Fig. 7. Plastic rotations were calculated from the moment–curvature diagrams, considering section geometry, material properties, and both longitudinal and transverse reinforcement ratios.

Different cracked section stiffness values were used for the design and evaluation stages. For the evaluation phase, the cracked section stiffnesses were determined in accordance with Section 5.4 of TBEC-2018. These values were obtained for all reinforced concrete members through moment–curvature analyses. For columns and shear walls, the stiffness values were calculated individually for each member, considering varying axial load levels, using the relevant formulation provided in the code. The yield moments of the sections were also determined based on the results of the moment–curvature analyses. Accordingly, deformation limits were defined based on these parameters. The damage states of the structural members were then determined for the limit performance levels specified in Chapter 5 of TBEC-2018, as shown in Fig. 8. In this figure, LD, CD, and CP represent Limited Damage, Controlled Damage, and Collapse Prevention performance levels, respectively. The intermediate regions, namely Limited Damage Region (LDR), Moderate Damage Region (MDR), Severe Damage Region (SDR), and Collapse Region (CR), were computed according to the plastic rotation and deformation demands of the structural elements.

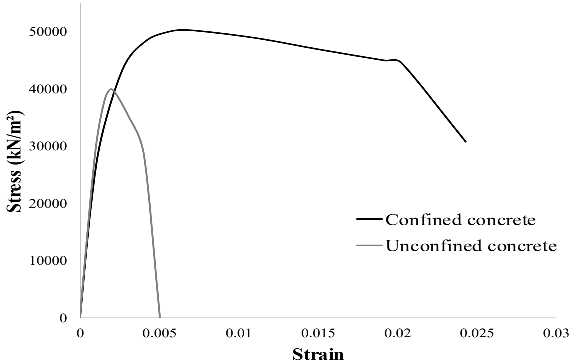

(a)

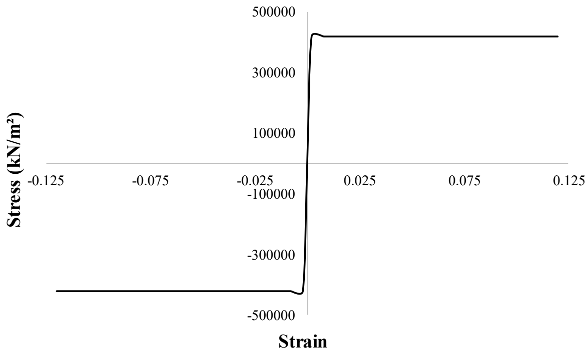

(b)

Fig. 7. Stress-strain relationships of materials. a) Stress-strain relationships of concrete and b) Stress-strain relationships of reinforcements

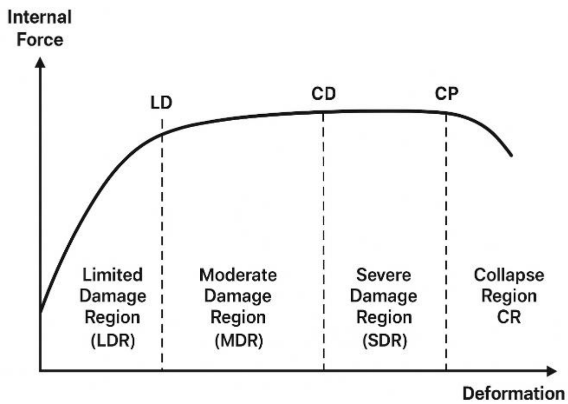

Fig. 8. Performance targets and damage regions

The plastic rotations of columns and beams were calculated using the moment–curvature relationships in accordance with Eqs. (2-4) defined in TBEC-2018. In these equations, L_p, L_s, and d_b represent the plastic hinge length, shear span, and longitudinal reinforcement diameter, respectively, while ϕ_u and ϕ_y denote the ultimate and yield curvatures. The deformation-based assessment specified by TBEC-2018 was carried out according to Eqs. (5–10).

$$\theta_p^{CP} = \frac{2}{3}\left[(\phi_u - \phi_y)L_p\left(1 - 0.5\frac{L_p}{L_s}\right) + 4.5\phi_u d_b\right] \tag{2}$$

$$\theta_p^{CD} = 0.75\theta_p^{CP} \tag{3}$$

$$\theta_p^{LD} = 0 \tag{4}$$

$$\varepsilon_c^{CP} = 0.0035 + 0.04\sqrt{w_{we}} \leq 0.018 \tag{5}$$

$$w_{we} = \alpha_{se}\rho_{sh,min}\frac{f_{ywe}}{f_{ce}} \tag{6}$$

$$\alpha_{se} = \left(1 - \frac{\sum a_i^2}{6b_o h_o}\right)\left(1 - \frac{s}{2b_o}\right)\left(1 - \frac{s}{2h_o}\right); \quad \rho_{sh} = \frac{2A_{sh}}{b_k s} \tag{7}$$

$$\varepsilon_s^{CP} = 0.40\varepsilon_{su} \tag{8}$$

$$\varepsilon_c^{CD} = 0.75\varepsilon_c^{CP}; \quad \varepsilon_s^{CD} = 0.75\varepsilon_s^{CP} \tag{9}$$

$$\varepsilon_c^{LD} = 0.0025; \quad \varepsilon_s^{LD} = 0.0075 \tag{10}$$

where, ε_C and ε_S indicate the strain values in concrete and steel, respectively; f_{ce} and f_{ywe}represent the concrete strength and the yield strength of the transverse reinforcement. The parameter αse denotes the effectiveness coefficient of the confinement reinforcement, and $\rho_{sh,min}$ corresponds to the minimum transverse reinforcement ratio in two horizontal directions. A_{sh} refers to the area of transverse reinforcement, and ρsh denotes its volumetric ratio. The parameters b_k and s represent the core concrete dimension and transverse reinforcement spacing, respectively, while b_o and h_o define the dimensions of the confined core section measured between the axes of the confining stirrups. Additionally, α_i represents the spacing between the longitudinal reinforcement bars restrained by a single stirrup leg or cross-tie. According to Eq. (2) of TBEC-2018, the plastic rotation corresponding to the Collapse Prevention (CP) performance level was calculated as 0.026 rad and 0.027 rad for columns with cross-sectional dimensions of 130×130 cm and 100×100 cm, respectively. Similarly, the limit plastic rotation for beams was found to be 0.038 rad. For shear walls, the limit state was defined in terms of deformation rather than rotation. The ultimate deformation limits corresponding to the Collapse Prevention performance level were determined as $\varepsilon_c = 0.012$ for the strain of confined concrete and $\varepsilon_s = 0.032$ for reinforcement steel.

In the analyses, each of the 11 earthquake records was applied in the X-direction, and the arithmetic mean of the obtained responses was considered. The resulting displacements, interstory drifts, and plastic rotations were compared with the code-specified limits to evaluate the overall structural performance. During the assessment, shear walls were evaluated based on plastic deformations, while columns and beams were evaluated according to plastic rotations, as specified in Chapter 5 of TBEC-2018. Damage distributions of the structural members were determined accordingly. Considering that damage concentration is typically more significant along the critical height of shear walls, the structural performance evaluation was conducted over this region. Based on TBEC-2018 provisions, the critical shear wall height depends on the total building height; in this study, it was taken as the first five stories, corresponding to a height of 15 meters.

3. Results and discussion

In this section, the structural response of a 27-story reinforced concrete high-rise building modeled in accordance with the provisions of TBEC-2018 is comparatively evaluated under both scaled and unscaled earthquake records. The analyses were conducted using the Nonlinear Time History Analysis (NTHA) method, and the structural behavior was assessed based on five key parameters: (i) Base shear forces, (ii) Roof and story displacements, (iii) Interstory drift ratios, (iv) Damage distribution in structural members, and (v) Strain distribution in shear walls.

According to the results presented in Table 4, the roof displacements increased by approximately 30% on average when scaled earthquake records were used, while the base shear forces exhibited only about 2% variation. This indicates that although scaling amplifies the input ground motion amplitudes, the ductile behavior of the structure limits the increase in base shear demand. Conversely, deformation and displacement demands in the upper stories become more pronounced. Particularly for the Northridge and L'Aquila records, an increase of up to 30% in base shear was observed after scaling, which can be attributed to the spectral content approaching resonance with the building’s fundamental period. Consequently, scaled records enhance the building’s energy dissipation capacity but also lead to significant increases in deformation demands.

Table 5 presents the results for story displacements and interstory drift ratios. The average interstory drift ratio was $\delta = 0.005$ for unscaled analyses and $\delta = 0.007$ for scaled analyses. According to TBEC-2018, the limit for interstory drift under DD-1 (maximum considered earthquake) level for high-rise buildings is 0.02 rad, and both cases remained within this limit. However, after scaling, the drift ratio increased by approximately 40–60% from the 5th story upward. This suggests that scaled records induce larger displacement differences in the mid and upper stories, implying that stiffness distribution and modal participation are highly sensitive to the seismic input characteristics. The increase in displacements in the upper stories may lead to the amplification of second-order (P-Δ) effects, which are of critical importance for defining performance limits in nonlinear analyses.

Table 4. Analysis result of base shear forces and top displacements

Earthquakes	Non-scaled		Scaled	
	Base shear force (kN)	Top displacement (m)	Base shear force (kN)	Top displacement (m)
Kocaeli	65667	0.374	67319	0.395
Bingol	67956	0.402	50136	0.562
ChiChi	63791	0.321	50136	0.420
Duzce	66535	0.376	67266	0.392
Elmayor6051	63791	0.381	50310	0.498
Elmayor6056	69608	0.412	52189	0.567
Erzincan	83258	0.353	74013	0.409
Landers	61761	0.442	54463	0.516
Loma Prieta	45430	0.324	74013	0.544
Northridge	59017	0.391	83224	0.568
L-Aquila	73717	0.351	96938	0.476
Average	64078	0.375	65455	0.486

Table 5. Interstory drift ratios

Story	Story height	Non-scaled			Scaled		
		Displacement (m)	Difference Δ (m)	Drift δ	Displacement (m)	Difference Δ (m)	Drift δ
1	3	0	0	0.000	0	0	0.000
2	3	0.0023	0.0023	0.001	0.003	0.003	0.001
3	3	0.0093	0.0069	0.002	0.012	0.009	0.003
4	3	0.0193	0.0100	0.003	0.025	0.013	0.004
5	3	0.0316	0.0123	0.004	0.041	0.016	0.005
6	3	0.0509	0.0193	0.006	0.066	0.025	0.008
7	3	0.0733	0.0224	0.007	0.095	0.029	0.010
8	3	0.0880	0.0147	0.005	0.114	0.019	0.006
9	3	0.1034	0.0154	0.005	0.134	0.020	0.007
10	3	0.1196	0.0162	0.005	0.155	0.021	0.007
11	3	0.1358	0.0162	0.005	0.176	0.021	0.007
12	3	0.1512	0.0154	0.005	0.196	0.020	0.007
13	3	0.1674	0.0162	0.005	0.217	0.021	0.007
14	3	0.1836	0.0162	0.005	0.238	0.021	0.007
15	3	0.1998	0.0162	0.005	0.259	0.021	0.007
16	3	0.2160	0.0162	0.005	0.280	0.021	0.007
17	3	0.2323	0.0162	0.005	0.301	0.021	0.007
18	3	0.2485	0.0162	0.005	0.322	0.021	0.007
19	3	0.2647	0.0162	0.005	0.343	0.021	0.007
20	3	0.2809	0.0162	0.005	0.364	0.021	0.007
21	3	0.2971	0.0162	0.005	0.385	0.021	0.007
22	3	0.3133	0.0162	0.005	0.406	0.021	0.007
23	3	0.3295	0.0162	0.005	0.427	0.021	0.007
24	3	0.3457	0.0162	0.005	0.448	0.021	0.007
25	3	0.3610	0.0153	0.005	0.469	0.021	0.007

As illustrated in Fig. 9(a), the relationship between roof displacement and story number indicates that scaled earthquake records significantly amplify the displacement response of the structure. In the scaled analyses, the roof displacement reached approximately 0.55 m, compared to 0.45 m for the unscaled cases—corresponding to an increase of around 22%. The primary reason for this increase is that scaling adjusts the spectral acceleration values of the records to better match the design spectrum near the structure's dominant period, leading to a more realistic representation of seismic energy input and consequently higher deformation demands. Examination of the slope differences in the roof displacement curves reveals that the scaled records produce steeper gradients, especially in the upper stories. This can be attributed to increased modal participation of higher modes, indicating that scaling influences not only the amplitude of the structural response but also the distribution of modal energy.

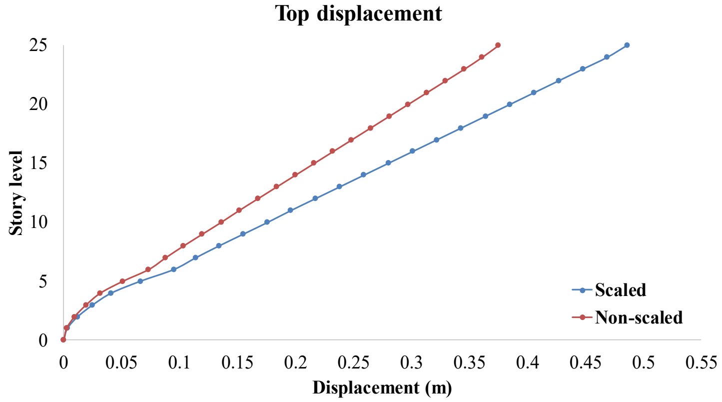

(a)

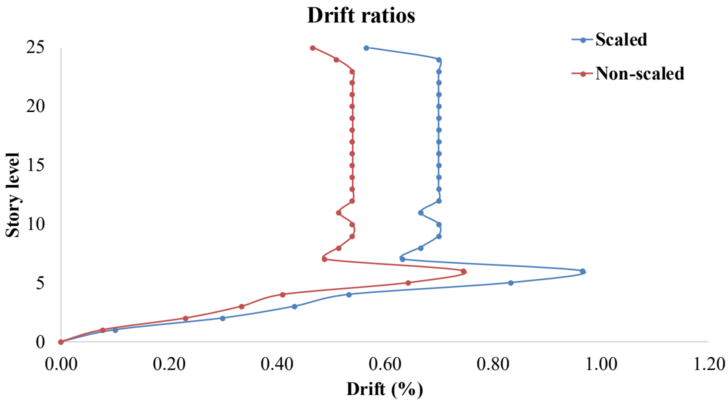

(b)

Fig. 9. a) Displacement and b) story drift ratios according to the story level

Fig. 9(b) shows the relationship between interstory drift ratio and story number, revealing that scaled earthquake records similarly lead to greater horizontal deformation demands. The story drift ratio (δ), used as one of the primary performance indicators, was calculated as the difference in lateral displacement (Δ) between two consecutive stories divided by the corresponding story height. While the drift ratios are comparable in the lower stories for both cases, the differences grow significantly in the mid and upper stories, reaching 0.8% in the scaled analyses—approximately 40–50% higher than the unscaled results. Moreover, the shape of the curve obtained from the scaled analyses is smoother and more linear in the lower stories, but becomes more irregular in the upper stories. These fluctuations arise from the interaction between stiffness discontinuities (soft-story effects) and mass distribution under seismic excitation. Although all values remain below the code limit of $\delta/h \leq 0.02$, the observed increases highlight the necessity of accounting for P–Δ effects in the seismic performance assessment of high-rise buildings. In summary, the analytical results presented in Fig. 9 clearly demonstrate that scaling earthquake records significantly amplifies displacement and drift demands in high-rise buildings. Therefore, proper implementation of the performance-based design approach prescribed by TBEC-2018 is essential. The adjustment of scaled records to the target design spectrum improves both the safety and realism of the analysis results.

Based on Table 6, scaling resulted in an average increase of 25–30% in both the major-axis and shear strain components of the shear walls, while the changes in the minor-axis direction were negligible. This demonstrates that the higher amplitude acceleration components after scaling become more effective along the principal direction of the shear walls. The maximum compressive strain values in the walls (εc ≈ 0.008–0.009) remained below the confinement limit of 0.012 specified by TBEC-2018 for the Collapse Prevention (CP) performance level of confined concrete. Therefore, it can be concluded that although the Controlled Damage (CD) performance level was exceeded, the structure did not reach collapse. This finding confirms that while scaling enhances the overall energy absorption capacity of high-rise structures, it also accentuates local damage in individual structural elements.

Finally, Fig. 10 illustrates the distribution of structural damage along the critical height of the shear wall under both scaled and unscaled earthquake records. The results clearly demonstrate that scaling the earthquake records alters not only the magnitude but also the spatial distribution of damage along the height of the structure. In the analyses performed with unscaled records, the majority of plastic rotations and compressive strain concentrations were confined to the first three stories, indicating a localized damage accumulation pattern near the base of the structure.

Table 6. Maximum strain values of reinforced concrete shear walls

Earthquakes	Non-scaled			Scaled		
	Minor axes	Major axes	Shear	Minor axes	Major axes	Shear
Kocaeli	0.0001	0.0070	0.0003	0.0001	0.0074	0.0003
Bingol	0.0001	0.0027	0.0002	0.0001	0.0038	0.0003
ChiChi	0.0001	0.0031	0.0002	0.0001	0.0041	0.0003
Duzce	0.0001	0.0030	0.0002	0.0001	0.0031	0.0002
Elmayor6051	0.0001	0.0034	0.0002	0.0001	0.0044	0.0002
Elmayor6056	0.0001	0.0035	0.0001	0.0001	0.0048	0.0002
Erzincan	0.0001	0.0067	0.0003	0.0001	0.0078	0.0003
Landers	0.0001	0.0058	0.0003	0.0001	0.0068	0.0003
Loma Prieta	0.0001	0.0038	0.0003	0.0002	0.0064	0.0005
Northridge	0.0000	0.0016	0.0001	0.0000	0.0023	0.0002
L-Aquila	0.0001	0.0062	0.0003	0.0002	0.0084	0.0004
Average	0.0007	0.0049	0.0002	0.0009	0.0064	0.0003

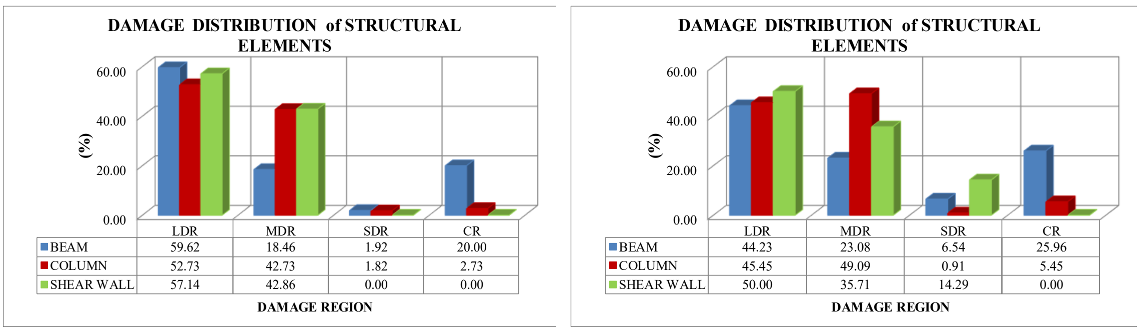

(a) (b)

Fig. 10. Distribution of structural damage along the critical height of the shear wall: a) Non-scaled and b) Scaled

After scaling, however, the intensity and extent of the damage region increased noticeably, spreading upward through approximately the first five stories. The concentration of plastic deformation was found predominantly within the first five stories, indicating that the lower-story walls function as the primary energy-dissipating components in high-rise structures, where most of the nonlinear behavior develops. After scaling, the regions of plastic rotation and deformation expanded upward, leading to a broader distribution of seismic energy along the height of the building.

Consequently, scaling promotes a more widespread ductile response, enhancing the overall energy dissipation capacity while providing a more realistic representation of nonlinear behavior in tall buildings. This behavior highlights a key implication of earthquake record scaling: although the structural performance level remains within the Controlled Damage (CD) range, the localized plastic strain intensity diminishes slightly due to a more extensive spread of deformation energy. In contrast, unscaled analyses produce narrower but more concentrated zones of plastic demand, which may result in earlier material degradation or local stiffness reduction. Thus, record scaling not only affects the quantitative response parameters—such as base shear or displacement—but also qualitatively transforms the damage pattern and the mechanism of energy dissipation within the structure.

4. Conclusion

This study investigated the seismic behavior of a 27-story reinforced concrete high-rise building modeled according to the Turkish Building Earthquake Code (TBEC-2018) under both scaled and unscaled ground motion records. Nonlinear time-history analyses were conducted to examine the influence of record scaling on key structural response parameters, including base shear, displacement demand, interstory drift ratios, and local damage distributions.

The results revealed that scaling substantially increases deformation demands while producing minor variations in base shear. Average roof displacements rose by approximately 30%, and interstory drift ratios increased by 40–60%, though all values remained within TBEC-2018 limits. The scaled analyses also led to a broader distribution of plastic deformations, extending damage from the lower to mid-story regions.

For reinforced concrete shear walls, both axial and shear strain components increased by about 25–30% under scaled records, yet compressive strain values remained below the collapse prevention threshold. Consequently, the overall performance level of the structure corresponded to the Controlled Damage (CD) range.

In summary, earthquake record scaling plays a decisive role in accurately capturing the nonlinear response and energy dissipation behavior of high-rise reinforced concrete buildings. Incorporating properly scaled ground motions in performance-based seismic assessment ensures more realistic and reliable predictions of structural behavior under severe earthquakes.

CRediT authorship contribution statement

Gokhan Dok: Writing – original draft, Visualization, Software, Conceptualization, Methodology, Investigation, Supervision, Writing – review & editing. Ali Bertu Saglam: Writing – review & editing, Conceptualization, Investigation, Methodology.

Declaration of conflicting interests

The author(s) declared no potential conflicts of interest with respect to the research, authorship, and/or publication of this article.

Funding

No funding was received for this study.

Data availability statement

The authors declare that there is currently no data availability in the list. Data availability information is not applicable.

References

[1] Disaster and Emergency Management Authority (2018) Turkish building earthquake code (TBEC-2018). AFAD, Ankara, Türkiye.
[2] Disaster and Emergency Management Authority (2025) Türkiye earthquake hazard map and parameters. AFAD, Ankara, Türkiye.
[3] Boğaziçi University Kandilli Observatory and Earthquake Research Institute (2021) Türkiye earthquake zones report. Kandilli Observatory and Earthquake Research Institute, Istanbul, Türkiye.
[4] Chopra AK (2012) Dynamics of structures: Theory and applications to earthquake engineering, 4th edn. Prentice Hall, Upper Saddle River.
[5] Priestley MJN, Calvi GM, Kowalsky MJ (2007) Displacement-based seismic design of structures. IUSS Press, Pavia.
[6] Fardis MN (2009) Seismic design, assessment and retrofitting of concrete buildings. Springer, Dordrecht.
[7] Yakut A (2019) Evaluation of new Turkish seismic code for reinforced concrete buildings. Bull Earthq Eng 17(6):3319–3340. https://doi.org/10.1007/s10518-019-00581-5
[8] Sezen H, Whittaker AS (2019) Performance-based seismic engineering in modern codes. Eng Struct 190:280–294. https://doi.org/10.1016/j.engstruct.2019.04.055
[9] Karakaş M, Yakut A (2020) Dynamic response of high-rise reinforced concrete buildings under near-fault ground motions. Earthq Struct 19(1):17–29.
[10] Elnashai AS, Di Sarno L (2015) Fundamentals of earthquake engineering. Wiley, Chichester.
[11] Hancock J, Bommer JJ (2006) A state-of-knowledge review of the selection and scaling of ground motion time histories. Earthq Spectra 22(2):625–653.
[12] Pacific Earthquake Engineering Research Center (PEER) (2019) Strong ground motion database. University of California, Berkeley.
[13] Kalkan E, Chopra AK (2010) Practical guidelines to select and scale earthquake records for nonlinear response history analysis of structures. Earthq Spectra 26(4):1237–1259.
[14] Lin TC, Miranda E (2020) Evaluation of ground motion scaling methods for performance-based design. Soil Dyn Earthq Eng 133:106095.
[15] Haselton CB, Deierlein GG (2007) Assessing seismic collapse safety of modern reinforced concrete moment-frame buildings. PEER Report 2007/08, University of California, Berkeley.
[16] Akkar S, Sandıkkaya MA, Bommer JJ (2014) Empirical ground-motion models for point- and extended-source crustal earthquake scenarios in Europe and the Middle East. Bull Earthq Eng 12:359–387.
[17] Duman T, Doğangün A (2021) Evaluation of nonlinear behavior of RC buildings using scaled ground motions. Soil Dyn Earthq Eng 143:106612.
[18] Fédération Internationale du Béton (FIB) (2010) Model code for concrete structures 2010. FIB, Lausanne.
[19] Chopra AK, McKenna F (2016) Modeling and analysis of structural systems subjected to earthquake ground motion. J Struct Eng 142(5):04016020.
[20] Öztürk H, Dok G, Karaalioğlu O (2024) Investigation of the effect of effective section stiffnesses defined in different codes on structural behavior. Erciyes Univ J Sci Inst 40(2):205–214.
[21] Computers and Structures Inc. (2023) SAP2000: Structural analysis and design, Version 23. Computers and Structures Inc., Berkeley, CA, USA.
[22] Dok G, Öztürk H, Demir A, Çağlar N (2020) Investigation of effective bending rigidity considering different code approaches. Acad Platform J Nat Hazards Disaster Manag 1(1):35–48.

[23] Das S, Choudhury S (2019) Influence of effective stiffness on the performance of RC frame buildings designed using displacement-based method and evaluation of column effective stiffness using ANN. Eng Struct 197:109354.

[24] Çağlar N, Demir A, Öztürk H, Akkaya A (2015) A simple formulation for effective flexural stiffness of circular reinforced concrete columns. Eng Appl Artif Intell 38:79–87.

[25] Özdemir Z, Fahjan YM (2007) Comparison of scaling methods of real earthquake records in time and frequency domains according to design spectra. In: Proc 6th Natl Conf Earthq Eng. Istanbul, Türkiye, 16–20 Oct, pp. 435–446.

[26] Turkish Standards Institution (TSE) (1997) TS 498: Design loads for buildings. TSE, Ankara, Türkiye.

[27] Pacific Earthquake Engineering Research Center (PEER) (2005) PEER strong motion database online. University of California, Berkeley. https://peer.berkeley.edu/peer-strong-ground-motion-databases

[28] Disaster and Emergency Management Authority (AFAD) (2025) TADAS – strong ground motion archive of the earthquake department of Türkiye. AFAD, Ankara, Türkiye. https://tadas.afad.gov.tr

[29] Imbsen Software Systems (2010) XTRACT: Cross-sectional structural analysis of components, Version 3.0. Imbsen Software Systems, Sacramento, CA, USA.